Cardiovasc Intervent Radiol (2013) 36:773–782
DOI 10.1007/s00270-012-0497-7

CIRSE

LABORATORY INVESTIGATION

Superselective Particle Embolization Enhances Efficacy of Radiofrequency Ablation: Effects of Particle Size and Sequence of Action

Toshihiro Tanaka · Peter Isfort · Till Braunschweig · Saskia Westphal · Anna Woitok · Tobias Penzkofer · Philipp Bruners · Kimihiko Kichikawa · Thomas Schmitz-Rode · Andreas H. Mahnken

Received: 19 June 2012 / Accepted: 7 September 2012 / Published online: 17 October 2012

Abstract
Purpose To evaluate the effects of particle size and course of action of superselective bland transcatheter arterial embolization (TAE) on the efficacy of radiofrequency ablation (RFA).
Methods Twenty pigs were divided into five groups: group 1a, 40-μm bland TAE before RFA; group 1b, 40-μm bland TAE after RFA; group 2a, 250-μm bland TAE before RFA; group 2b, 250-μm bland TAE after RFA and group 3, RFA alone. A total of 40 treatments were performed with a combined CT and angiography system. The sizes of the treated zones were measured from contrast-enhanced CTs on days 1 and 28. Animals were humanely killed, and the treated zones were examined pathologically.
Results There were no complications during procedures and follow-up. The short-axis diameter of the ablation zone in group 1a (mean ± standard deviation, 3.19 ± 0.39 cm) was significantly larger than in group 1b (2.44 ± 0.52 cm; $P = 0.021$), group 2a (2.51 ± 0.32 cm; $P = 0.048$), group 2b (2.19 ± 0.44 cm; $P = 0.02$), and group 3 (1.91 ± 0.55 cm; $P < 0.001$). The greatest volume of ablation was achieved by performing embolization with 40-μm particles before RFA (group 1a; 20.97 ± 9.65 cm^3). At histology, 40-μm microspheres were observed to occlude smaller and more distal arteries than 250-μm microspheres.
Conclusion Bland TAE is more effective before RFA than postablation embolization. The use of very small 40-μm microspheres enhances the efficacy of RFA more than the use of larger particles.

Keywords Embolization · Experimental interventional radiology · Interventional oncology · Radiofrequency ablation

T. Tanaka (✉) · K. Kichikawa
Department of Radiology, Nara Medical University, 840 Shijo-cho, Kashihara 634-8522, Japan
e-mail: toshihir@bf6.so-net.ne.jp

K. Kichikawa
e-mail: kkichika@naramed-u.ac.jp

T. Tanaka · P. Isfort · T. Penzkofer · P. Bruners · T. Schmitz-Rode · A. H. Mahnken
Applied Medical Engineering, Helmholtz-Institute Aachen, RWTH Aachen University, Aachen, Germany
e-mail: isfort@hia.rwth-aachen.de

T. Penzkofer
e-mail: penzkofer@rad.rwth-aachen.de

P. Bruners
e-mail: bruners@rad.rwth-aachen.de

T. Schmitz-Rode
e-mail: smiro@hia.rwth-aachen.de

A. H. Mahnken
e-mail: mahnken@rad.rwth-aachen.de

P. Isfort · T. Penzkofer · P. Bruners · A. H. Mahnken
Department of Diagnostic and Interventional Radiology, Aachen University Hospital, RWTH Aachen University, Aachen, Germany

T. Braunschweig · S. Westphal
Department of Pathology, Aachen University Hospital, RWTH Aachen University, Aachen, Germany
e-mail: tbraunschweig@ukaachen.de

S. Westphal
e-mail: swestphal@ukaachen.de

A. Woitok
Institute for Laboratory Animal Science, RWTH Aachen University, Aachen, Germany
e-mail: awoitok@ukaachen.de

Introduction

Minimally invasive image-guided treatments for liver cancer have been developing. Currently, radiofrequency ablation (RFA) is successfully used and plays an important role for the treatment of primary and metastatic liver tumors. The success of RFA is highly dependent on tumor size and the heat-sink effect [1, 2]. To overcome this problem, the combination therapy of RFA with transcatheter chemoembolization (TACE) has been introduced. Previous experimental studies demonstrated the advantage of TACE using iodized oil (lipiodol-TACE) followed by RFA, which achieved a larger coagulation volume compared with RFA alone [3, 4]. Several clinical studies demonstrated that the combination of RFA and lipiodol-TACE achieved similar results regarding overall survival when compared with surgical resection in patients with early stage hepatocellular carcinoma [5, 6]. Yet the benefit of combination therapy for hepatocellular carcinomas smaller than 3 cm is controversial [7]. However, the following limitations of the combination of lipiodol-TACE and RFA should be considered: lipiodol-TACE is less effective for hypovascular tumors (e.g., metastatic colorectal cancer) and chemoresistant tumors (e.g., metastatic neuroendocrine tumors) [8].

TACE after RFA in the same session is another treatment option, which was previously reported to enhance the efficacy of RFA [9]. This combination exploits the reactive hyperemia induced by RFA, thereby facilitating the delivery of an embolic agent into the tumor-bearing area.

Recently, precisely calibrated small-size microspheres with a diameter as small as 40 μm were developed and are now commercially available [10, 11]. Theoretically, bland transcatheter embolization (TAE) with these novel microspheres could achieve peripheral occlusion of the targeted arteries. Therefore, we hypothesized that bland TAE using 40-μm microspheres before RFA could either effectively devascularize the region of interest before RFA or effectively occlude the hypervascular reactive rim that typically occurs after RFA and thereby enhance the efficacy of RFA.

Because the best strategy with respect to particle size and course of action is not yet known, the goals of this experimental study were to investigate whether bland TAE that used very small microspheres enhances efficacy of RFA more than larger particles, and to determine the optimal treatment order.

Materials and Methods

Outline of Study Design

An animal study on the combination therapy of bland TAE using small microspheres and RFA was conducted. Twenty pigs were assigned to one of the following five treatments (four pigs per group): (1) bland TAE with 40-μm microspheres was conducted before RFA (group 1a), (2) bland TAE with 40-μm microspheres was conducted after RFA (group 1b), (3) bland TAE with 250-μm microspheres was conducted before RFA (group 2a), (4) bland TAE with 250-μm microspheres was conducted after RFA (group 2b), and (5) RFA alone was performed without any additional treatment (group 3). Each pig received two treatments in two different areas of the liver in a single treatment session. A total of 40 areas were treated. Two of the four pigs in each group were humanely killed 1 day after treatment (day 1), and the remaining two pigs were killed 28 days after treatment (day 28). All pigs underwent intravenous contrast-enhanced CT (ceCT) immediately before they were killed (Fig. 1). Lesion size and appearance were assessed from ceCT, and pathological analysis was conducted in all animals.

Animals

The study was approved by the state committee on animal affairs. A total of 20 female pigs weighing 60–63 kg (mean 61.5 kg) were used. After intramuscular premedication with 0.5 ml atropine 1 % (atropinum sulfuricum solution 1 %; WDT, Garbsen, Germany), 0.2 mg/kg azaperone (Stresnil; Janssen-Cilag, Neuss, Germany), and 5 mg/kg ketamine (ketamine 10 %; Ceva, Düsseldorf, Germany), anesthesia was induced by intravenous injection of diluted pentobarbital (Narcoren, Merial, Hallbergmoos, Germany). All animals were orotracheally intubated and mechanically ventilated with an oxygen–air mixture containing 1.0 vol% isoflurane (Abbott, Baar, Switzerland) at a respiratory rate of 15 breaths/min. For pain management, 0.01 mg/kg buprenorphin (Temgesic; Essex Pharma, Munich, Germany) was administered intramuscularly.

Interventional Procedures

All interventional procedures were performed with a dual-source CT scanner (Somatom Definition, Siemens, Forchheim, Germany) in combination with a mobile C-arm-based angiography system (Arcadis Orbic 3D; Siemens, Forchheim, Germany). The C arm was positioned in the gap between the CT gantry and the scanner table, which allowed for performing CT scans and the digital subtraction angiograms on the same table without moving the pigs during the experiments.

Pigs were positioned supine on the CT table, and a nonenhanced CT scan was performed with a standardized examination protocol as follows: 64 × 0.6 mm collimation; 120 kV tube voltage, 220 mAs_{eff} effective tube current–time product, pitch 0.9.

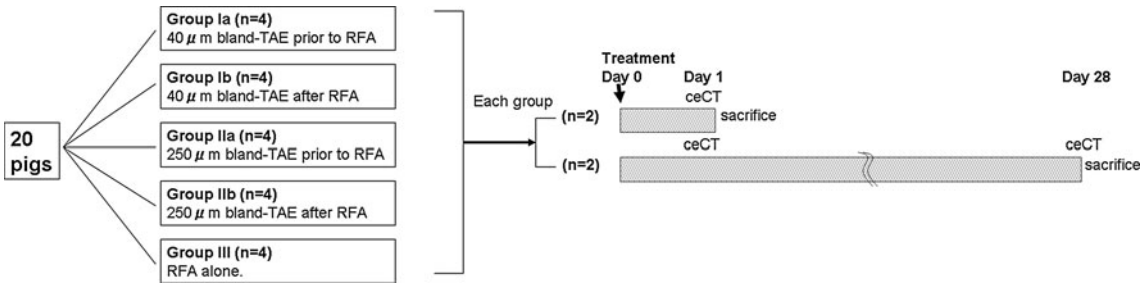

Fig. 1 Study design and treatment schedule. Each pig received two treatments in two different areas

For angiographic procedures, the right iliac artery was percutaneously punctured with an 18-gauge needle; then a 5F introducer sheath (Pinnacle introducer; Terumo, Tokyo, Japan) was inserted. Under fluoroscopic guidance, a 5F cobra-shaped angiographic catheter was inserted into the celiac trunk, and a celiac angiogram was obtained by injection of 20 ml of iopromide 370 at an injection rate of 5 ml/s (Fig. 2A). According to morphological findings of the liver on the initial CT, the sites of treatments were determined. Basically, two sites were chosen in the left and right parts of the liver. However, when the left part was atrophic ($n = 4$), both treatments were conducted in the right part, and when the stomach or colon was positioned between the skin puncture site and the right part ($n = 2$), both treatments were conducted in the left part. By the coaxial method, a 2.6F-tip microcatheter (Nadeshiko; JMS, Tokyo, Japan) was inserted superselectively into one of the peripheral hepatic arterial branches in the targeted hepatic lobe. After the superselective angiography was obtained, CT during arterial injection of contrast material via the microcatheter (5 ml iopromide 370 injected at 0.5 ml/s) was performed (Fig. 2B, C). On the basis of this superselective intraarterial ceCT, an expandable electrode with 2-cm array diameter (LeVeen; Boston Scientific, Natick, MA, USA) was placed in the center of the contrast-enhanced area. Actual electrode placements were performed under CT guidance using a sequential imaging mode with the following scan parameters: 12 × 12 mm collimation, 50 mAs_{eff} effective tube current–time product, 120 kV tube voltage, and 2.4-mm slice thickness. After the radiofrequency (RF) electrode was properly placed and the probe was expanded, a superselective intraarterial ceCT was obtained to confirm that all prongs were placed completely inside the contrast-enhanced area (Fig. 2D).

In groups 1a and 2a, bland TAE was conducted before RFA. Calibrated 40-μm or 250-μm microspheres (Embozene; CeloNova BioSciences, Newnan, GA, USA) were used. A vial of microspheres containing 2-ml particles suspended in 5 ml of carrier solution was mixed with 13 ml of iopromide 370. The microspheres were slowly injected for 10 min via the microcatheter with a 1-ml syringe. The end point of embolization was stasis of the flow in the targeted hepatic arterial branch for at least 5 s. Approximately 1 min after bland TAE, RFA was performed. After four grounding pads were placed on the back and the upper limbs, the probe and the grounding pads were connected with a commercially available monopolar RF generator (RF 3000; Boston Scientific). A two-phase energy application protocol, as recommended by the manufacturer, was applied. In the first phase, the initial output was set to 30 W and increased by 10 W every minute up to a maximum of 60 W; this energy level was maintained until tissue impedance increased by 500 Ω ("roll-off"). After a 30-s pause, a second phase started at half of the maximum power of the first phase. After 5 min, the power was increased by 10 W per minute up to a maximum of 60 W. RFA was finished when the second roll-off occurred.

In groups 1b and 2b, RFA was conducted before bland TAE applying the same ablation protocol as described above. Fifteen minutes after the end of ablation, bland TAE with 40-μm (group 1b) or 250-μm (group 2b) microspheres was performed using the same technique as in groups 1a and 2a. In group 3, RFA without embolization was performed using the same protocol.

After all RFA and TAE procedures, the catheter and the introducer sheath were removed and the puncture site was occluded by the use of a vessel closure device (Starclose; Abbott, Des Plaines, IL, USA).

Imaging

For follow-up, arterial and venous phase ceCT were performed with the same CT scanner and examination protocol as for the baseline scan. For contrast enhancement, 123 ml of iopromide 370 followed by a 30-ml saline bolus was injected via an ear vein at a flow rate of 3.3 ml/s. For contrast timing, the bolus tracking method was used, with a region of interest placed in the abdominal aorta at the level of celiac trunk. The arterial phase scan was started 13 s after a threshold of 140 HU was reached in the region of interest. The venous phase scan was started 45 s after the arterial phase scan was completed. The CT data were transferred to an external workstation equipped with a

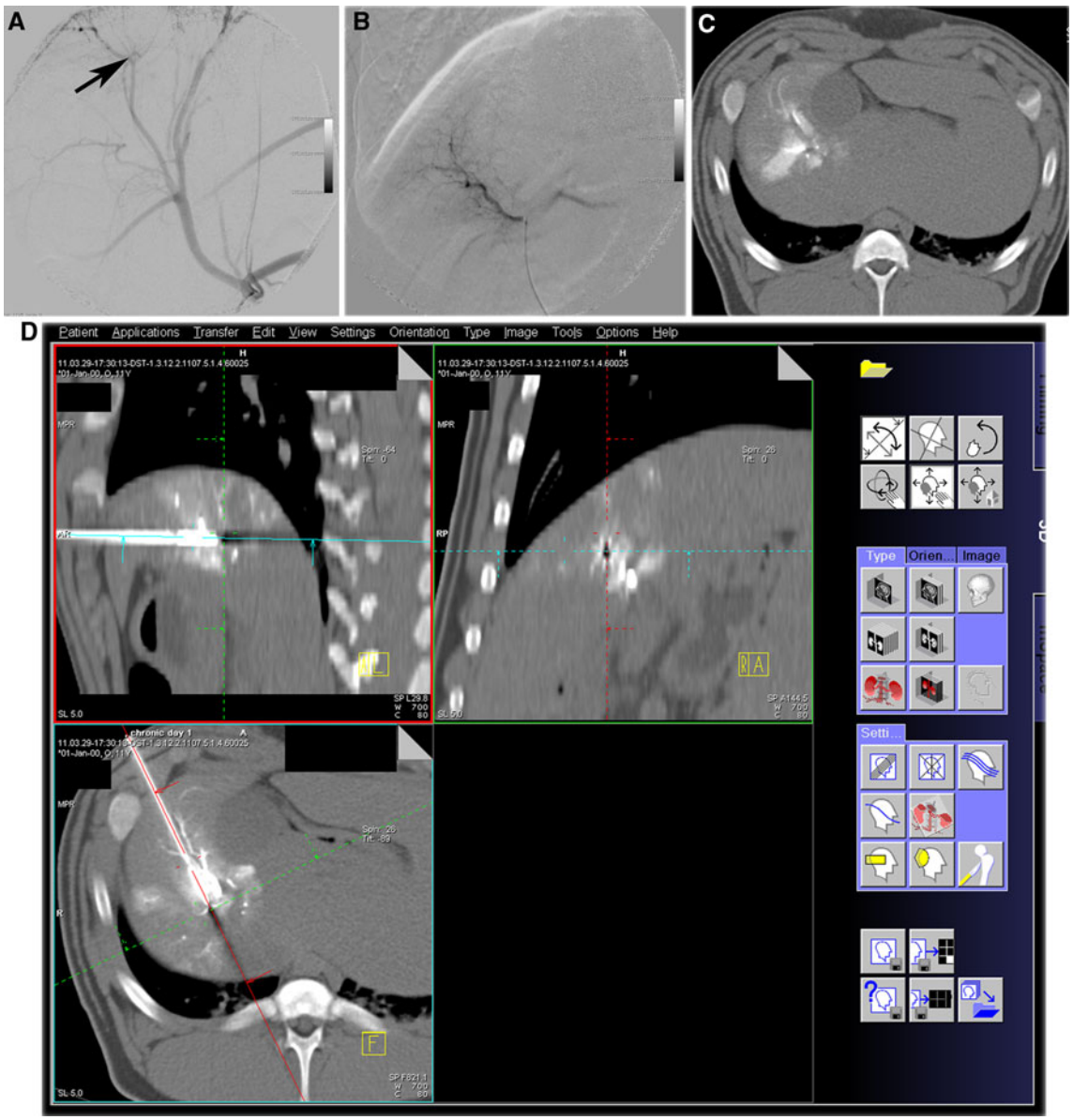

Fig. 2 **A** Celiac arteriography via a 5F catheter. A microcatheter was inserted into a branch of the right hepatic artery, which was supplying into the anterior–superior segment of the right part of the liver (*arrow*). **B** Superselective arteriography via the microcatheter. **C** CT during arterial injection of contrast material via the microcatheter. **D** In 3D-CT imaging after the RF electrode insertion, all expandable arrays of a RF electrode are placed inside the enhanced area via the microcatheter

dedicated software tool (MMWP; Siemens Medical Solution) for data evaluation.

The ablation sizes were evaluated according to the standard terminology and reporting criteria for image-guided tumor ablation [12]. An unenhanced low-attenuation area on the ceCT was defined as the ablation zone. The wedge-shaped, relatively low-attenuation area peripherally spreading from the ablation zone was defined as the peripheral infarction zone, which corresponds to areas of hepatic infarction according to Morimoto et al. [13]. The ablation and peripheral infarction zones were manually outlined in each CT slice, and volumetric analysis was performed by software (Syngo Oncology; Siemens Medical Solution). The short-axis diameters and volumes of ablation were evaluated from ceCT on days 1 and 28. The volume of the peripheral infarction zone was calculated from ceCT on day 1.

Pathologic Evaluation

Immediately after an animal had been humanely killed, total hepatectomy was performed, and the liver was fixed in a 10 % buffered formalin solution. After complete fixation for at least 24 h, the liver was sectioned axially in

5-mm cuts. Tissue samples were embedded in paraffin and cut into 2–3-μm thin sections placed glass slides. After rehydration, the sections were stained with hematoxylin and eosin for microscopic examination. The widths of the marginal rims (hemorrhagic rims) that surrounded the coagulation zones were measured.

Statistical Analysis

All data were provided as mathematical mean ± standard deviation. A one-way analysis of variance adjusted for multiple testing according to Bonferroni was performed to analyze the ablation duration, the short-axis diameter and volume of the ablation zone, the volume of the peripheral infarction zone, and the width of the marginal rim for statistically significant differences between each group. A *P*-value of less than 0.05 was considered statistically significant. Data were analyzed by SPSS II, version 17.0 (SPSS, Chicago, IL, USA).

Results

A total of 40 treatments were successfully performed without any early or delayed complications. All pigs survived the follow-up time according to our study protocol. In 14 pigs, the two ablated sites were in the right and left parts of the liver, in four pigs only in the right part (2 in group 1b, 1 in group 2a, and 1 in group 3), and in two pigs only in the left part (one each in groups 1a and 2a). In all of the combination therapies, the expanded arrays of RF electrodes were successfully placed inside the target areas in all animals. The mean injected volume of the diluted microspheres per treatment was 5.5 ml. The average ablation duration was 989 ± 340 s in group 1a, 1173 ± 365 s in group 1b, 1187 ± 238 s in group 2a, 906 ± 191 s in group 2b, and 1081 ± 109 s in group 3. There were no significant differences in ablation duration between the different groups.

Size of Ablation Zone and Peripheral Infarction Zone

The ablation zones and peripheral infarction zones could easily be distinguished from each other and from the surrounding normal liver tissue (Fig. 3). The short-axis diameter, the volume and marginal rim of the ablation zone, and the volume of peripheral infarction zone on day 1 are listed in Table 1. The ablated short-axis diameter of group 1a was significantly larger than that of group 1b ($P = 0.021$), group 2a ($P = 0.048$), group 2b ($P = 0.02$), and group 3 ($P < 0.001$). The ablated volume of group 1a was significantly larger than that of group 3 ($P = 0.008$). The peripheral infarction zones were found in all treatment zones in groups 1a and 2a, in 7 (87.5 %) of 8 treatment zones in group 1b, and in 6 (75 %) of 8 treatment zones in group 2b. In group 3, the peripheral infarction zone was not seen.

Pathological Findings 1 Day after Treatment

At histology, all ablation zones consisted of a coagulation zone and a hemorrhagic rim (Fig. 4). In the coagulation zones, hepatocytes with dense basophilic nuclei and amorphous eosinophilic stained cytoplasm were seen. In the hemorrhagic rims, infiltration of lymphocytes and macrophages, as well as less affected hepatocytes next to hemorrhage were seen (Fig. 5). There were no visible differences in the appearances of the ablation zones of each group. The mean widths of hemorrhagic rims are provided in Table 1. Although there were no statistically significant differences in these values, the hemorrhagic rims' widths tended to be thicker in group 1b (Fig. 4). In the peripheral infarction zones, more regression effects in liver parenchyma were seen, presenting necrosis and congestion.

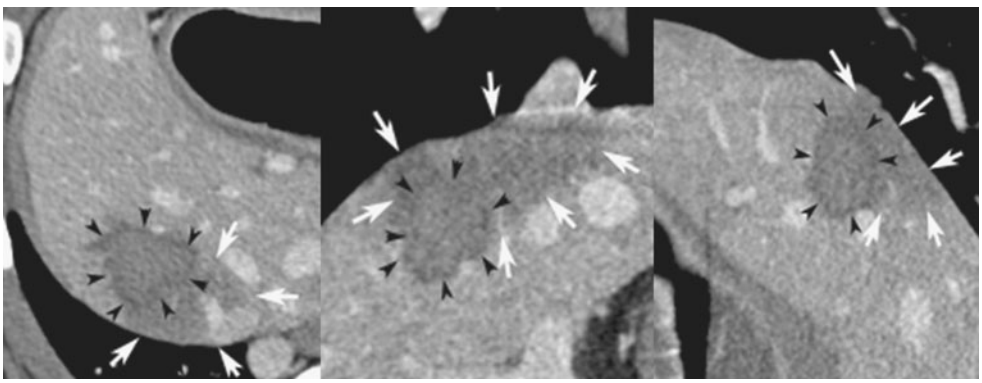

Fig. 3 Contrast-enhanced CT obtained 1 day after the combined treatment of 40-μm bland TAE before RFA (group 1a) via 3D-reconstruction imaging (axial, sagittal, and coronal images). The ablation zone is depicted as nonenhanced low-density area (*black arrowhead*). The peripheral infarction zone is depicted as the wedge-shaped low-density areas peripherally spreading from the ablation zones (*white arrow*)

Table 1 Comparison of short-axis diameter, volume and marginal rim of ablation zone, and volume of peripheral infarction zone on day 1

Group	Ablation short-axis diameter (cm)	Ablation volume (cm^3)	Peripheral infarction volume (cm^3)	Marginal rim (cm)
1a	3.19 ± 0.39[a,b,c,d]	20.97 ± 9.65[d]	19.7 ± 22.83	0.35 ± 0.06
1b	2.44 ± 0.52[e]	15.17 ± 4.79	13.5 ± 18.95	0.62 ± 0.43
2a	2.51 ± 0.32[e]	14.97 ± 7.17	22.9 ± 15.94	0.23 ± 0.05
2b	2.19 ± 0.44[e]	12.38 ± 4.34	20.0 ± 24.82	0.25 ± 0.05
3	1.91 ± 0.55[e]	8.83 ± 4.73[e]	–	0.30 ± 0.08

Data are expressed as mean ± standard deviation

[a] Significant difference in comparison to group 1b

[b] Significant difference in comparison to group 2a

[c] Significant difference in comparison to group 2b

[d] Significant difference in comparison to group 3. Significant differences in repeated measures analysis of variance are indicated

[e] Significant difference in comparison to group 1a

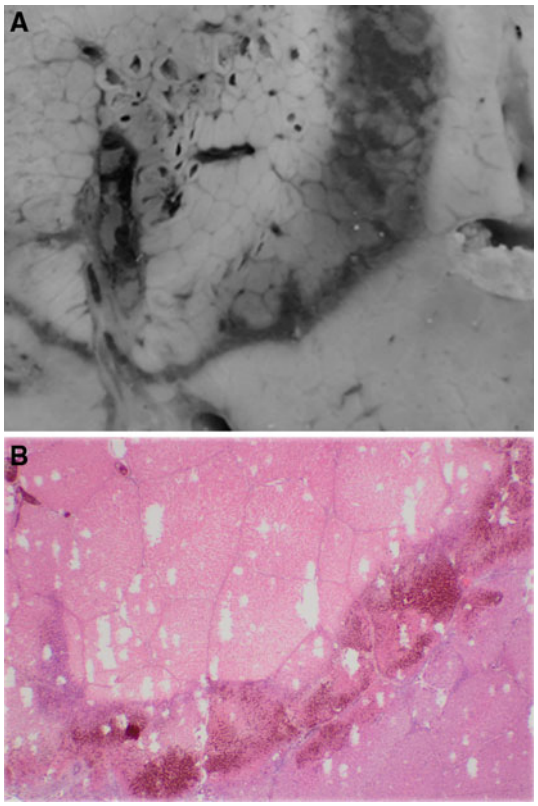

Fig. 4 Ablation zone obtained 1 day after the combined treatment of 40-μm bland TAE after RFA (group 1b). **A** Gross examination reveals a *gray* central coagulation zone (*upper left*) surrounded by a relatively thick dark marginal rim, representing hemorrhage. **B** Coagulation zone (*upper left*) is separated from normal tissue (*lower right*) by the hemorrhagic rim (hematoxylin and eosin, original magnification ×2.5)

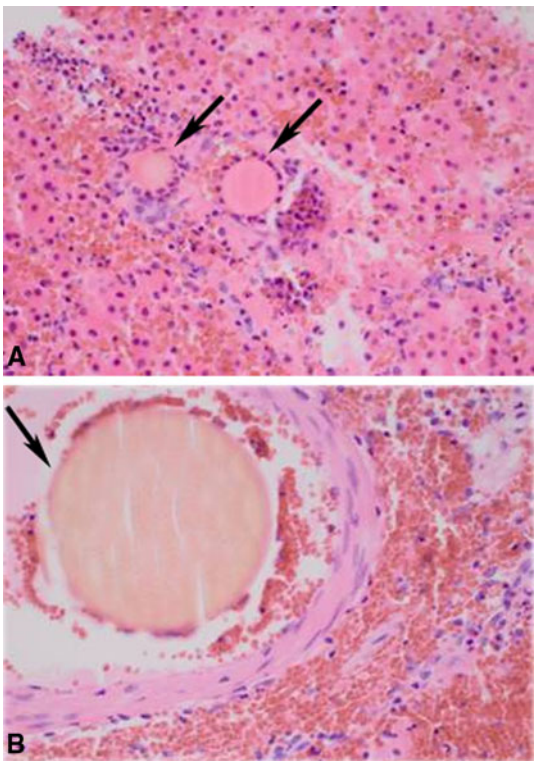

Fig. 5 Microscopic examination of the hemorrhagic rims (original magnification ×40). **A** A 40-μm bland TAE before RFA (group 1a) revealed infiltration of lymphocytes and macrophages, and necrotic hepatocytes with hemorrhage are present. The microspheres are present in the small arteries and arterioles. **B** A 250-μm bland TAE before RFA (group 2a) revealed microspheres present in lower numbers and in relatively large arteries

These findings were observed in all groups except group 3. In the area around the ablation zone in cases where bland TAE alone was performed, the microspheres were visible in small vessels, showing focal inflammation but not necrotic effects in the adjacent tissue.

Changes of the CT Imaging and Pathological Findings 28 Days after Treatment

The short-axis diameters, and the volumes and marginal rim sizes of the ablation zones on day 28 are provided in Table 2. There were no significant differences in these

Table 2 Comparison of short-axis diameter, and volume and marginal rim of ablation zone on day 28

Group	Ablation short-axis diameter (cm)	Ablation volume (cm^3)	Marginal rim (cm)
1a	1.70 ± 0.26	3.23 ± 0.89	0.13 ± 0.05
1b	1.59 ± 0.73	2.71 ± 1.40	0.23 ± 005
2a	1.53 ± 0.17	2.68 ± 1.48	0.18 ± 0.05
2b	1.49 ± 0.88	2.37 ± 1.18	0.15 ± 0.06
3	1.56 ± 0.40	2.82 ± 0.46	0.16 ± 0.06

Data are expressed as mean ± standard deviation

values between the different groups. At pathologic analysis on day 28, the coagulation zones exhibited signs of organization of the necrosis compared with day 1. The marginal rims changed to thinner fibrous tissue in which macrophages and giant cells were often present facing to the necrotic center of the lesion. The spherical microspheres were still seen without any deformation at the same vascular levels as on day 1, but they were often surrounded by giant cells and lymphocytes, indicating a foreign-body reaction (Fig. 6).

Comparison Between Bland TAE Before and After RFA

When comparing the ablation size between groups 1a and 1b, the short-axis diameter of group 1a on day 1 was significantly larger than in group 1b ($P = 0.021$). In contrast, there were no significant differences between groups 2a and 2b. At microscopy, there were no microspheres in the coagulation zones of groups 1b and 2b, whereas deformed microspheres were seen in the coagulation zones of groups 1a and 2a. The heat of RFA caused the microspheres to collapse, thereby losing their spherical shape.

Effect of Microsphere Size

When comparing the size of ablation between groups 1a and 2a (in these groups, bland TAE was performed before RFA), the short-axis diameters of group 1a on the ceCT on day 1 were significantly larger than those of group 2a ($P = 0.048$). In comparison, there were no significant differences between groups 1b and 2b, although the mean short-axis diameters and marginal rim widths of group 1b tended to be larger than those of group 2b. At microscopic examination, 40-µm microspheres were seen to occlude remarkably in smaller arteries when compared with 250-µm microspheres (Fig. 5). The 40-µm microspheres were frequently seen in the marginal rims in group 1b, whereas 250-µm microspheres were rarely seen in this location in group 2b (Fig. 6).

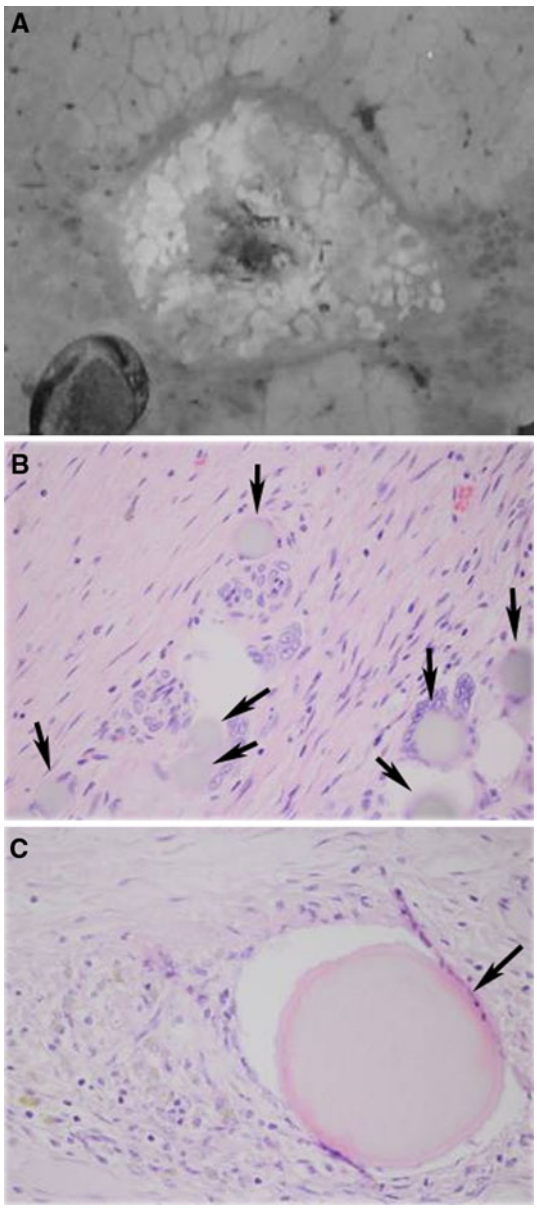

Fig. 6 Ablation zone obtained 28 days after the combined treatment of bland TAE after RFA. **A** Gross examination (group 1b) revealed a *gray* central coagulation zone surrounded by a thin, fibrotic marginal rim. **B** A 40-µm bland TAE after RFA (group 1b) revealing fibrous tissue of the marginal rim in which macrophages and giant cells surrounding the microspheres are present (original magnification ×40). The microspheres are often present without any deformation in the small arteries. No microspheres could be detected within the necrotic center of the lesion. **C** A 250-µm bland TAE after RFA (group 2b) revealed that microspheres are rarely present without any deformation in the relatively large arteries (original magnification ×40)

Discussion

This is the first experimental study to demonstrate the superior effectiveness of 40-µm microspheres over larger particles in the combination of bland TAE and RFA.

Previously, several in vivo experimental studies demonstrated that lipiodol-TACE before RFA achieved a larger coagulation volume compared with RFA alone, whereas bland TAE before RFA did not; Sugimori et al. and Iwamoto et al. used 1-mm gelatin sponge particles, and Mostafa et al. used 300-μm microspheres [3, 14, 15]. They both noted that proximal embolization with gelatin sponge particles and microspheres induced the collateral blood supply into the treatment area, which did not prevent the blood-cooling effect for RFA. In our study, very small and precisely calibrated microspheres were used. Our results demonstrated that the ablation zone produced by bland TAE with 40-μm microspheres before RFA was significantly larger in all groups. From these results, it can be assumed that precisely calibrated 40-μm microspheres traveled more distally into small vessels, thereby increasing the heat retention during RFA.

To investigate the effective sizes of microspheres for bland TAE before RFA is an important issue. In our study, 40-μm microspheres produced a significantly larger ablation size compared with 250-μm microspheres, and 250-μm microspheres did not achieve a significantly larger ablation size when compared with RFA alone. At microscopy, 40-μm microspheres were present in markedly smaller arteries and arterioles compared with 250-μm microspheres. Although we examined only two sizes of microspheres, our results indicated that microspheres smaller than 250 μm appear to be effective for the use of bland TAE before RFA. Recently, Bonomo et al. [16] reported their initial clinical experiences of bland TAE with calibrated 100-μm microspheres before RFA of liver metastases; theirs was the first report regarding the combination therapy of RFA and bland TAE. Their study demonstrated a large ablated diameter (median 59.5 mm) and a high complete response rate (96.7 %). The findings of this study concur with the results reported by Bonomo and coworkers, indicating the improved effectiveness if calibrated small particles are used for preablation bland TAE.

The concepts of bland TAE after RFA in the same session were another key issue addressed in our study. Previously, Lencioni et al. [9] proposed TACE with drug-eluting beads after RFA. The theoretical benefit of this combination order is that bland TAE or TACE could destroy the residual cancer cells at the tumor periphery after RFA. Intraarterial administration of chemotherapy after RFA might be an efficient strategy because many kinds of chemotherapy are not stable in the heat when they are administered before RFA. On the other hand, the aim of bland TAE with small microspheres immediately after RFA is to occlude arterial flows peripherally in the hypervascular reactive rim produced by RFA. In our study, many microspheres were found in the marginal rims (hemorrhagic rims), and the widths of the marginal rims were relatively thicker when compared with those of RFA alone. These results support the hypothesis that bland TAE with small microspheres after RFA could increase the antitumoral effect in the periablational zone. Regarding the effective sizes of microspheres, at microscopic examination, 250-μm microspheres were rarely seen in the marginal rims, whereas 40-μm microspheres were frequently seen. This suggests that 40-μm microspheres could be more effective compared with 250-μm microspheres in bland TAE after RFA, as well as bland TAE before RFA.

Peripheral infarction zones were observed under ceCT at the periphery of the liver adjacent to the ablation zone in the combination groups. The mechanism of the peripheral infarction is still unclear. Previously, Morimoto et al. [13] reported that lipiodol-TAE produced peripheral infarction zones, whereas bland TAE with gelatin sponge particles did not. They noted that the dual occlusion of the hepatic arteries and the portal veins by lipiodol might induce this phenomenon. However, the microscopic findings in our study demonstrated that the microspheres were present only in the hepatic arteries and arterioles, but not in the portal veins. From this result, the following mechanism could be considered: the RFA damaged the small branches of the portal veins and the microspheres occluded the hepatic arteries, which might have produced peripheral infarction and hemorrhage.

Forty microns is the smallest size of currently commercially available microspheres. To our knowledge, ours is the first report to describe the combination of bland TAE with 40-μm microspheres and RFA in an animal model. In our study, the animals survived without any complications for at least 4 weeks. When using 40-μm microspheres, the possibility of complications like liver dysfunction and pulmonary infarction resulting from nontarget embolization due to the presence of hepatic shunts must be kept in mind [17]. In particular, there is a high risk of developing shunts after puncture with the RF electrode. Therefore, a careful angiographic evaluation is mandatory before embolization. Superselective catheterization will limit the embolization effects to tumor tissue, thereby helping to prevent liver dysfunction by sparing non-tumor-bearing tissue. This experimental animal study was conducted with a CT and angiography system under similar conditions as those used for the treatment of humans. A hybrid CT and angiography system is useful for conducting superselective TAE because the embolization area was precisely estimated before TAE by CT during contrast injection via a microcatheter [18]. Another advantage of a CT and angiography system is that CT-guided RFA and angiography could be conducted on the same table without having to move the subject.

In our study, bland TAE and RFA were performed consecutively during the same session. The ideal time interval

between TAE/TACE and RFA is unknown. Yamakado et al. [5] and Kagawa et al. [6] performed RFA during the 2 weeks and 2 months, respectively, after lipiodol-TACE. In contrast, Bonomo et al. [16] performed RFA immediately after bland TAE. The following benefits in performing the combination therapy within the same session were considered: (1) the certainty of achieving a distinct heat retention effect without recanalization of the arterial flow and development of new collateral blood supplies; (2) the ease in managing any bleeding that may occur during RFA; and (3) the shortening of the length of hospital stay for patients. However, the risk of liver dysfunction is unclear. Further clinical studies are required to evaluate the safety of the combination therapy during the same session.

The combination of bland TAE using small microspheres and RFA appears to be a promising treatment for hypovascular liver tumors—for example, metastatic colorectal cancer. The treatment of RFA for metastatic colorectal cancer is challenging. RFA alone is known to go along with a local recurrence rate ranging from approximately 9–40 %, most likely due to an insufficient safety margin around the area of ablation [19–23]. Because metastatic colorectal cancer is supplied from fine feeding vessels [24], precisely calibrated small microspheres could occlude these fine vessels distally and thus should be effective in providing an adequate degree of ischemia.

High-risk patients with poor liver function could be promising candidates for this combination therapy. TACE, performed with an emulsion of lipiodol and chemotherapy or with drug-eluting beads, increases the likelihood of liver toxicity and damage to this organ [8, 25]. Bland TAE should have milder toxicity than TACE [26]; however, caution must be taken when small-size microspheres are used because they may carry the risk of severe complications, such as pulmonary embolism, as a result of shunt passage of the small beads [17].

There were several limitations to this study. First, healthy pig livers without tumors were treated. Second, as a result of the limited number of animals, we used only two sizes of microspheres. Further investigations that use other currently commercially available 75- and 100-μm microspheres are necessary.

In conclusion, our experimental study demonstrated that RFA combined with superselective bland TAE using 40-μm microspheres enhances the efficacy of RFA. Particle size influenced results, with bland TAE using 40-μm microspheres before RFA being the most effective. Clinical trials for patients with liver cancer are warranted to assess the novel therapeutic strategy of superselective bland TAE using 40-μm microspheres before RFA.

Acknowledgments The authors acknowledge the advice of Marian Pahud (Valkenburg, The Netherlands).

Conflict of interest This study was sponsored in parts by CeloNova Bio-Sciences, San Antonio, TX, USA. This work was among the 10 % best-rated scientific papers at CIRSE 2012, and we were invited to submit it here. The authors declare that they have no conflict of interest.

References

1. Goldberg SN, Hahn PF, Tanabe KK et al (1998) Percutaneous radiofrequency tissue ablation: does perfusion-mediated tissue cooling limit coagulation necrosis? J Vasc Interv Radiol 9:101–111
2. Bleicher RJ, Allegra DP, Nora DT et al (2003) Radiofrequency ablation in 447 complex unresectable liver tumors: lessons learned. Ann Surg Oncol 10:52–58
3. Mostafa EM, Ganguli S, Faintuch S et al (2008) Optimal strategies for combining transcatheter arterial chemoembolization and radiofrequency ablation in rabbit VX2 hepatic tumors. J Vasc Interv Radiol 19:1740–1748
4. Nakai M, Sato M, Sahara S et al (2007) Radiofrequency ablation in a porcine liver model: effects of transcatheter arterial embolization with iodized oil on ablation time, maximum output, and coagulation diameter as well as angiographic characteristics. World J Gastroenterol 13:2841–2845
5. Yamakado K, Nakatsuka A, Takaki H et al (2008) Early-stage hepatocellular carcinoma: radiofrequency ablation combined with chemoembolization versus hepatectomy. Radiology 247:260–266
6. Kagawa T, Koizumi J, Kojima S, et al; Tokai RFA Study Group (2010) Transcatheter arterial chemoembolization plus radiofrequency ablation therapy for early stage hepatocellular carcinoma: comparison with surgical resection Cancer 116:3638–3644
7. Shibata T, Isoda H, Hirokawa Y et al (2009) Small hepatocellular carcinoma: is radiofrequency ablation combined with transcatheter arterial chemoembolization more effective than radiofrequency ablation alone for treatment? Radiology 252:905–913
8. Kim JH, Yoon HK, Ko GY et al (2010) Nonresectable combined hepatocellular carcinoma and cholangiocarcinoma: analysis of the response and prognostic factors after transcatheter arterial chemoembolization. Radiology 255:270–277
9. Lencioni R, Crocetti L, Petruzzi P et al (2008) Doxorubicin-eluting bead–enhanced radiofrequency ablation of hepatocellular carcinoma: a pilot clinical study. J Hepatol 49:217–222
10. Stampfl S, Bellemann N, Stampfl U et al (2009) Arterial distribution characteristics of Embozene particles and comparison with other spherical embolic agents in the porcine acute embolization model. J Vasc Interv Radiol 20:1597–1607
11. Bonomo G, Pedicini V, Monfardini L et al (2010) Bland embolization in patients with unresectable hepatocellular carcinoma using precise, tightly size-calibrated, anti-inflammatory microparticles: first clinical experience and one-year follow-up. Cardiovasc Intervent Radiol 33:552–559
12. Goldberg SN, Grassi CJ, Cardella JF et al (2005) Society of Interventional Radiology Technology Assessment Committee. Image-guided tumor ablation: standardization of terminology and reporting criteria. J Vasc Interv Radiol 16:765–778
13. Morimoto M, Numata K, Nozawa A et al (2010) Radiofrequency ablation of the liver: extended effect of transcatheter arterial embolization with iodized oil and gelatin sponge on histopathologic changes during follow-up in a pig model. J Vasc Interv Radiol 21:1716–1724
14. Sugimori K, Nozawa A, Morimoto M et al (2005) Extension of radiofrequency ablation of the liver by transcatheter arterial embolization with iodized oil and gelatin sponge: results in a pig model. J Vasc Interv Radiol 16:849–856

15. Iwamoto T, Kawai N, Sato M et al (2008) Effectiveness of hepatic arterial embolization on radiofrequency ablation volume in a swine model: relationship to portal venous flow and liver parenchymal pressure. J Vasc Interv Radiol 19:1646–1651
16. Bonomo G, Della Vigna P Monfardini L et al (2012) Combined therapies for the treatment of technically unresectable liver malignancies: bland embolization and radiofrequency thermal ablation within the same session. Cardiovasc Intervent Radiol. doi:10.1007/s00270-012-0341-0
17. Brown KT (2004) Fatal pulmonary complications after arterial embolization with 40–120-μm Tris–acryl gelatin microspheres. J Vasc Interv Radiol 15:197–200
18. Toyoda H, Kumada T, Sone Y (2009) Impact of a unified CT angiography system on outcome of patients with hepatocellular carcinoma. AJR Am J Roentgenol 192:766–774
19. Park IJ, Kim HC, Yu CS et al (2008) Radiofrequency ablation for metachronous liver metastasis from colorectal cancer after curative surgery. Ann Surg Oncol 15:227–232
20. Aloia TA, Vauthey JN, Loyer EM et al (2006) Solitary colorectal liver metastasis: resection determines outcome. Arch Surg 141: 460–466
21. Yoon HM, Kim JH, Shin YM et al (2012) Percutaneous radiofrequency ablation using internally cooled wet electrodes for treatment of colorectal liver metastases. Clin Radiol 67: 122–127
22. de Baere T, Elias D, Dromain C et al (2000) Radiofrequency ablation of 100 hepatic metastases with a mean follow-up of more than 1 year. Am J Roentgenol 175:1619–1625
23. Crocetti L, de Baere T, Lencioni R (2010) Quality improvement guidelines for radiofrequency ablation of liver tumors. Cardiovasc Intervent Radiol 33:11–17
24. de Baere T, Deschamps F (2011) Arterial therapies of colorectal cancer metastases to the liver. Abdom Imaging 36:661–670
25. Guiu B, Deschamps F, Aho S et al (2012) Liver/biliary injuries following chemoembolisation of endocrine tumours and hepatocellular carcinoma: lipiodol vs drug-eluting beads. J Hepatol 56:609–617
26. Lewis AL, Taylor RR, Hall B et al (2006) Pharmacokinetic and safety study of doxorubicin-eluting beads in a porcine model of hepatic arterial embolization. J Vasc Interv Radiol 17: 1335–1343